Inner Dynein Arms but Not Outer Dynein Arms Require the Activity of Kinesin Homologue Protein KHP1^{FLA10} to Reach the Distal Part of Flagella in *Chlamydomonas*

Gianni Piperno, Kara Mead, and Scott Henderson

Department of Cell Biology and Anatomy, Mount Sinai School of Medicine, New York 10029

Abstract. Inner dynein arms, but not outer dynein arms, require the activity of KHP1^{FLA10} to reach the distal part of axonemes before binding to outer doublet microtubules. We have analyzed the rescue of inner or outer dynein arms in quadriflagellate dikaryons by immunofluorescence microscopy of p28^{IDA4}, an inner dynein arm light chain, or IC69^{ODA6}, an outer dynein arm intermediate chain. In dikaryons two strains with different genetic backgrounds share the cytoplasm. As a consequence, wild-type axonemal precursors are transported to and assembled in mutant axonemes to complement the defects. The rescue of inner dynein arms containing p28 in *ida*4–wild-type dikaryons progressively occurred from the distal part of the axonemes and with time was extended towards the proximal part. In contrast, the rescue of outer dynein arms in *oda*2–wild-type dikaryons progressively occurred along the entire length of the axoneme. Rescue of inner dynein arms containing p28 in *ida*4*fla*10-*fla*10 dikaryons was similar to the rescue observed in *ida*4–wild-type dikaryons at 21°C, whereas it was inhibited at 32°C, a nonpermissive temperature for KHP1^{FLA10}. In contrast, rescue of outer dynein arms in *oda*2*fla*10-*fla*10 dikaryons was similar to the rescue observed in *oda*2–wild-type dikaryons at both 21° and 32°C and was not inhibited at 32°C. Positioning of substructures in the internal part of the axonemal shaft requires the activity of kinesin homologue protein 1.

Chlamydomonas flagella are a model system for the analysis of assembly and function of eukaryotic cilia and flagella. They are amenable to genetic analysis, and their structure and motility has been described in many details (19). Their motile component, the axoneme, contains >200 proteins at varying concentrations bound to the microtubule framework.

The majority of axonemal protein mass, including tubulin and two radial spoke subunits, reaches the distal part of developing axonemes before binding to the microtubule framework that is already completed (9). However, the group of proteins directly binding to the proximal part of the axonemes (35) and the pathway of assembly of axonemal substructures, such as dynein arms, "dynein regulatory complex" (28), and central pair complex, remain to be identified. The dynein arms, in particular, may be involved in a complex mechanism of transport and binding to the outer doublet microtubules as a consequence of their heterogeneity in composition and their diverse locations in the axonemes.

The dynein arms are required for the generation of ciliary and flagellar types of movement of *Chlamydomonas* flagella and are distinguished in seven groups. They include one type of outer dynein arm, which mainly influences the beat frequency of flagella (4), and six types of inner dynein arms (18), which mainly generate the waveforms of flagella (4). The outer dynein arms as well as one type of inner dynein arm (27) are uniformly distributed along the axoneme, whereas five types of inner dynein arms are asymmetrically distributed along and around the axoneme (12, 18, 26). In particular, two types of inner dynein arm heavy chains are formed late in the generation of flagella and are located only at the proximal part of the axoneme (26).

To identify a mechanism that differentiates time and site of binding of the inner dynein arms, we intended to determine whether inner and outer dynein arm subunits are transported within flagella to the distal end of the axoneme, like tubulin and radial spoke subunits. If inner dynein arms are transported to a part of the axoneme that is different from where outer dynein arms are transported, then we could begin to examine the molecular basis of their transport and binding to the outer doublet microtubules as possible causes of temporal and spatial differentiation.

Different types of transport of dynein precursors could indicate the existence of a sorting mechanism. Transport of precursors within the axoneme could occur by diffusion

Address all correspondence to Gianni Piperno, Mount Sinai School of Medicine, Department of Cell Biology and Anatomy, One Gustave L. Levy Place, Box 1007, New York, NY 10029-6574. Tel.: (212) 241-0773. Fax: (212) 860-1174.

© The Rockefeller University Press, 0021-9525/96/04/371/9 $2.00

or require the activity of a molecular motor. The identification of the kinesin homologue protein 1 (KHP1)[1] as an axonemal component has suggested the existence of an active transport of axonemal molecules toward the distal part of the axoneme (33). KHP1 is the product of the *FLA*10 locus and is similar to the kinesin KIF3 of mouse cerebellum (33). It is located between the axonemal outer doublet microtubules and the flagellar membrane (15). The activity of KHP1 is required for both bidirectional movement of polystyrene beads on the flagellar membrane and bidirectional movement of granule-like particles beneath the flagellar membrane (14, 15).

Here, we describe experiments devoted to identifying mode of transport and binding of dynein arms within the axoneme. We determined whether two dynein subunits require the activity of KHP1 for their transport within the axoneme. We selected p28, an inner dynein arm light chain (27), and IC69, an outer dynein arm intermediate chain (23), as target molecules. p28 is the product of *IDA*4 and is required for the assembly of two inner dynein arms, each including one specific inner dynein arm heavy chain and actin (17, 18). One of these inner dynein arms is located at the proximal part of the axoneme (26). IC69 is the product of *ODA*6 (23) and is missing from nearly all *oda* mutants together with the totality of outer dynein arms (11).

We approached the study of both the transport and binding of axonemal dynein arm subunits by the creation of quadriflagellated temporal dikaryons that allow structural and functional rescue of mutant flagella (21). In dikaryons two strains with different genetic backgrounds share their cytoplasm. As a consequence, wild-type axonemal precursors are transported to and assembled in mutant axonemes to complement mutant defects. Structural rescue of inner or outer dynein arms was observed before in *ida*4–wild-type (17) and *oda*2–wild-type (20) dikaryons, respectively. We detected p28 and IC69 in mutant axonemes of these dikaryons by immunofluorescence microscopy and specific antibodies.

Materials and Methods

Strains Used and Cell Culture Conditions

The strains *fla*10-1 (33) and *ida*4-1 (17, 18) were used for all experiments described below and are referred to as *fla*10 and *ida*4, respectively. The wild-type strains 137 and *fla*10 are from the collection of Dr. David Luck (Rockefeller University, New York). *oda*2, *oda*6, and *ida*4 were kindly provided by Dr. Ritsu Kamiya (University of Tokyo, Japan). The strain *fla*10 is temperature sensitive for flagellar assembly and carries a defective KHP1 protein (33). The strains *ida*4, *oda*2, and *oda*6 are defective for axonemal motility. *ida*4 lacks two types of inner dynein arm heavy chains from the axonemes and is a null mutant of p28. *oda*2 (34) and *oda*6 (23) lack all outer dynein arms from the axoneme and have the γ chain and IC69 of outer dynein arms as defective gene products, respectively. *FLA*10 is located in the left arm of the UNI linkage group; *ODA*6 and *IDA*4 are located in the left arm of linkage group XII/XIII, and *ODA*2 is in the right arm of linkage group XI. Recombinant strains *ida*4*fla*10 and *oda*2*fla*10 were isolated by standard procedures (6).

Gametes were grown on solid L medium (21) for 7 d (3 d at 25°C in bright light and 4 d at 21°C in the dark).

1. *Abbreviation used in this paper*: KHP1, kinesin homologue protein 1.

Immunofluorescence Microscopy

Gametic cells were resuspended in nitrogen-free medium at a density of 2–4 × 10^7 cells per ml and incubated at 21°C for 3 h. In some experiments gametes of opposite mating types were mated at both 21° and 32°C, and dikaryons were analyzed within 1 h after mating. Gametes were preincubated for 1 h with spent medium containing autolytic enzymes to release the cell wall (6). Resulting protoplasts from gametes or dikaryons were extracted by stirring in a rotary shaker at room temperature for 20 min in 6 vol of a solution containing 25% glycerol, 1% NP-40, 15 mM EGTA, 2.5 mM $MgCl_2$, 0.1 M Pipes, pH 6.7, and a few crystals of PMSF (16). 1-ml aliquots of the resulting suspension were treated with 2 vol of 3% formaldehyde in 0.1 M sodium phosphate, pH 6.8, at room temperature for 10 min. Extracted and fixed protoplasts were separated from unextracted cells by a centrifugation for 10 min at 1,200 rpm and 4°C in a rotor (GH-3.7; Beckman Instruments, Fullerton, CA). The supernatant was collected and centrifuged for 10 min at 3,000 rpm and 4°C. The pellet was resuspended in 30 μl of PBS (0.01 M sodium phosphate, 0.13 M NaCl, pH 6.8), and the suspension was layered on No. 1 glass coverslips (before use, coverslips were washed with PCA, rinsed with water, coated in 0.1 mg/ml poly-ornithine, and air dried). After 10 min, coverslips were washed and then covered with polyclonal antibodies specific for p28 (18) or mAb specific for IC69 (13) (Sigma Chemical Co., St. Louis, MO) for 1 h at room temperature. Dilutions were 1:1,000 (anti-p28) or 1:500 (anti-IC69) in PBS containing 1 mg/ml BSA. After washing, the coverslips were incubated in 1:200 or 1:600 dilutions of fluoresceinated anti–rabbit or anti–mouse antibodies (in PBS containing 1 mg/ml BSA) for 1 h at room temperature, washed, and mounted on a microscope slide. All washes were repeated three times in PBS for 10 min each. The mounting medium consisted of 9 vol of glycerol, 1 vol of 1 M Tris/HCl, pH 7, 1 mg/ml *p*-phenylenediamine, 25 mg/ml NaN_3.

The antibody specific for p28 cross-reacts with a 130,000 molecular weight protein that is a component of the cell wall (G. Piperno, unpublished results). This cross-reactivity does not affect the detection of p28 in axonemes and basal bodies (see Fig. 1) because gametes and dikaryons were deprived of the cell wall before being processed for immunofluorescence staining.

Specimens were examined by confocal laser scanning microscopy (CLSM; Leica GmbH, Heidelberg, Germany). Images of fluorescein labeling were acquired by excitation of the specimens with the λ = 488 line of a krypton/argon laser, using a KP510 short pass excitation filter, a double dichroic (488-, 568-nm) beam splitter, and a LP515 long pass barrier filter (Leica GmbH). Images of the entire protoplast were acquired by confocal detection of reflected light (KP590 short pass excitation filter, a neutral beam splitter, and no barrier filter). This method of detection exploits differences in refractive indices of the object studied and the surrounding media (24), and is capable of resolving individual microtubules (2).

Digitized records of immunofluorescence and reflectance images were collected only for dikaryons whose four flagella were in the same plane of focus. This subset of dikaryons represents a minority compared to the dikaryons that had at least one flagellum outside the plane of focus or lost one flagellum. Optical sections with a depth of field of ~0.5 μm were analyzed and could contain all four flagella in their full length (diameter and length of flagella are 0.2 and 11 μm, respectively). Parts of flagella in Figs. 3 *h*, 6 *d*, and 7 *b* are less contrasted against the background. This phenomenon depends on local differences of refractive index of the medium surrounding the flagella. Changing the focal plane did not provide more contrasted images.

Reflectance images of *Chlamydomonas* protoplasts, as they were obtained in glycerol mounting medium, were superior in definition and contrast to those obtained by conventional phase contrast microscopy.

Partial Purification of Basal Bodies

This was performed with a modification of the method of Snell (31). All centrifugations were at 4°C. Gametes were collected and washed once in nitrogen-free medium by centrifugation at 1,600 rpm in the GH-3.7 rotor. Cell pellets were resuspended in 100 ml of spent medium containing autolytic enzymes and stirred at room temperature for 30 min. After a release from the cell wall, protoplasts were deprived of flagella by pH shock, centrifuged as above, and washed in 10 mM Tris/HCl, 1 mM EDTA, pH 7.5 (TE) by centrifugation at 2,000 rpm in the GH-3.7 rotor. Pellets were deprived of excess liquid and resuspended in 50 ml of spent medium containing autolytic enzymes and 1% NP-40. After 10 min, crystals of PMSF were added, and protoplasts were lysed by 10 strokes in a glass/glass homogeneizer at 0°C. The lysate was layered over 17 ml of 25% sucrose in

two disposable 50-ml tubes and centrifuged 10 min at 2,000 rpm in the GH-3.7 rotor. The supernatant was overlaid in 45-ml polycarbonate tubes over three sucrose layers (formed by 6-ml 30%, 6-ml 40%, and 6-ml 50% sucrose in TE) and centrifuged 60 min at 10,500 rpm in the HB.4 rotor (Sorvall Instruments Div.; Dupont, Wilmington, DE). The 40% sucrose layer, which is yellow due to the presence of cellular debris, was collected, diluted 1:1 with TE, layered over three sucrose layers (formed by 5-ml 50%, 5-ml 55%, and 5-ml 60% sucrose in TE), and centifuged for 120 min at 10,500 rpm in the HB.4 rotor. A white band between the 50% and the 55% layer was collected, diluted 1:1 with TE, and centrifuged 30 min at 17,000 rpm in a SS-34 rotor (Sorvall Instruments Div.; Dupont, Wilmington, DE). Basal bodies formed a transparent pellet that also contained cell wall fragments.

Protein Analysis

SDS gel electrophoresis was performed as described (18). Proteins were transferred electrophoretically to an Immobilon membrane in a buffer consisting of 10 mM 3-cyclohexylamino-1-propanesulfonic acid (CAPS), 10% methanol, pH 11.0. After transfer, some of the membranes were stained with 0.1% Coomassie blue in 50% methanol, 10% acetic acid, and destained in 50% methanol, 10% acetic acid. Western blot analysis was performed using a chemiluminescence kit from Amersham Corp. (Arlington Heights, IL) following the manufacturer's instructions. The primary antiserum was typically diluted 5,000-fold, and the secondary antibody 10,000-fold.

Results

Detection of Inner and Outer Dynein Arm Subunits in Chlamydomonas Axonemes

To determine whether the antibodies specific for p28, the inner dynein arm light chain, and IC69, the outer dynein arm intermediate chain, are suitable for the immunofluorescence microscopy of *Chlamydomonas* axonemes, we extracted and fixed wild-type protoplasts before exposing them to each antibody.

Each antibody bound to antigens located along the axoneme but did not bind to the transition zone between axonemes and basal bodies that do not contain dynein arms (Fig. 1, *a* and *b*, and *e* and *f*, respectively). The antibody specific for p28 also bound to the basal bodies that were separated from each other by a region that did not contain the antigen (Fig. 1 *a*, *inset*). In contrast, the antibody specific for IC69 did not bind to the basal bodies (Fig. 1 *e*).

The antibodies against p28 did not bind axonemes or basal bodies in protoplasts of *ida*4, a null mutant of p28 (Fig. 1, *c* and *d*). Furthermore, the antibodies specific for IC69 did not bind axonemes of *oda*2, a mutant lacking all outer dynein arms (not shown), or axonemes of *oda*2 in dikaryons (see Figs. 4 *a* and 8 *a*). Therefore, each antibody specifically stained axonemes in wild-type protoplasts.

Presence of p28 in Basal Bodies

To confirm that the basal bodies contain p28, we prepared and analyzed subcellular fractions enriched in basal bodies and deprived of axonemes from wild-type cells. We compared the proteins present in basal bodies to those present in the axonemes by Western blots (Fig. 2). Three blots, each containing proteins from basal body and axoneme fractions, were prepared in parallel and incubated with antibodies specific for p28, α-tubulin, and outer dynein arm γ chain, respectively (Fig. 2, *a–c*). The antibodies specific for p28 bound to proteins of molecular weight close to 28,000 in both basal body and axoneme fractions (Fig. 2 *c*). The

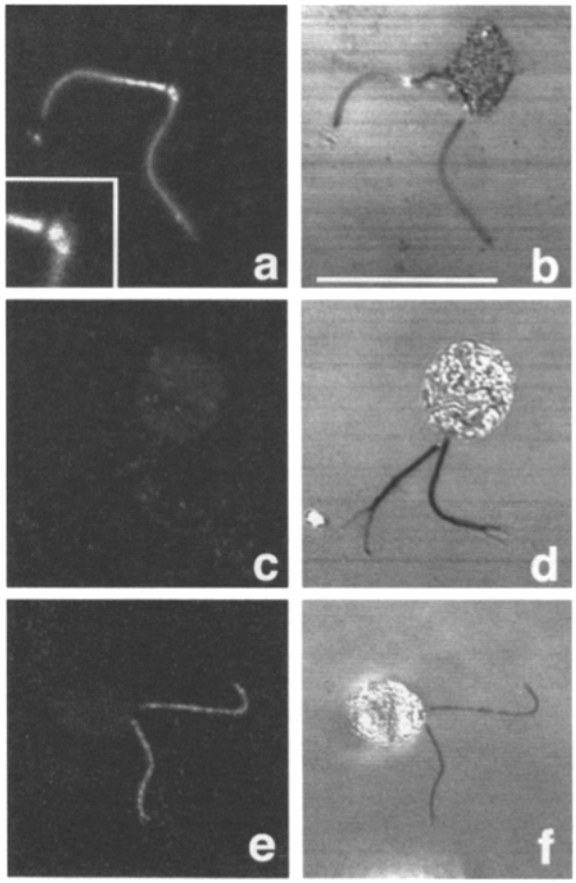

Figure 1. Immunofluorescence staining of wild-type (*a*) and (*e*) and *ida*4 protoplasts (*c*), as detected by confocal laser scanning microscopy. (*a*) Wild-type axonemes and basal bodies are stained by polyclonal antibodies specific for p28. (*c*) Neither axonemes nor basal bodies are stained in *ida*4, a null mutant of p28, by polyclonal antibodies specific for p28. (*e*) Wild-type axonemes, but not basal bodies, are stained by an mAb specific for IC69. (*b*, *d*, and *f*) Corresponding images generated by reflectance confocal scanning laser microscopy. Inset in *a* shows discontinuous staining between the basal bodies and in the transition region between axonemes and basal bodies (~×2). Bar, 10 μm.

antibody specific for α-tubulin bound to similar amounts of antigens in both basal body and axoneme fractions (Fig. 2 *b*). In contrast, the antibody specific for outer dynein arm γ chain bound to the antigen only in the axonemal fraction (Fig. 2 *a*). Therefore, the basal body fraction contained p28 and tubulin like the axonemal fraction but was not contaminated with axonemes.

Binding of the Inner Dynein Arm Subunit p28 at the Distal Part of the Axoneme

To determine whether p28 binds to the outer doublet microtubules at the distal part of the axoneme, we created quadriflagellated temporary dikaryons by mating a wild-type strain to *ida*4, a p28 null mutant (18). At 6, 20, 30, and 60 min after mating, we tested for the presence of p28 in the dikaryons by immunofluorescence microscopy (Fig. 3).

The antigen was present in one pair of axonemes, presumably the wild-type pair, in dikaryons extracted at 6 min after mating (Fig. 3, *a* and *b*). It was detected at the distal

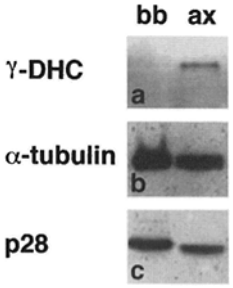

Figure 2. Western blot analysis of basal body and axoneme proteins from a wild-type strain. (*a*) Immunostaining by the mAb 277-27 specific for the outer dynein arm heavy chain γ. (*b*) Immunostaining by the mAb B-5-1-2 specific for α-tubulin. (*c*) Immunostaining by polyclonal antibodies specific for p28.

but not at the proximal part of *ida*4 axonemes at 20 and 30 min after mating (Fig. 3, *c* and *d*, and *e* and *f*, respectively). Distal and proximal part of *ida*4 axonemes were stained with approximately the same intensity at 60 min after mating (Fig. 3, *g* and *h*). A strong immunofluorescent signal derived from the presence of p28 in *ida*4 basal bodies (Fig. 3 *a*, *inset*), was detected at least 10 min before a weak signal derived from the binding of p28 in *ida*4 axonemes could be detected.

The images shown in Fig. 3 were selected as typical examples of the 52 images collected in six independent experiments. 32 of these images were collected between 15 and 30 min after mating, and all showed clear evidence of preferential p28 binding at the distal end of *ida*4 axonemes. Dikaryons shown in Fig. 3 were prepared at 32°C. Parallel experiments performed at 21°C showed that kinetics and sites of binding of p28 in *ida*4 basal bodies and axonemes were not changed within the 21–32°C range of temperature.

This evidence indicates that the structures containing p28 are rescued from the distal part of mutant axonemes in *ida*4–wild-type dikaryons. Furthermore, the binding of p28 to the basal bodies is faster than that observed for the axonemes.

Binding of the Outer Dynein Arm Subunit IC69 along the Axoneme

To determine whether IC69, the outer dynein arm intermediate chain, binds to the outer doublet microtubules at the distal part of the axoneme, we created quadriflagellated temporary dikaryons by mating a wild-type strain to *oda*2, an outer armless mutant (11). At 6, 30, and 60 min after mating at 32°C, we detected the presence of IC69 in the dikaryons by immunofluorescence microscopy (Fig. 4).

The antigen was undetectable in the pair of mutant axonemes at 6 min after mating (Fig. 4 *a*), but it was evident at 30 and 60 min (Fig. 4, *c* and *e*). Both distal and proximal parts of mutant axonemes were stained with similar intensity at 30 and 60 min (Fig. 4, *c* and *e*, respectively). At 20 min after mating, the amount of IC69 bound to the pair of mutant axonemes was lower but still occurred along the entire length of the axoneme (not shown). The images shown in Fig. 4 were selected as typical examples of the 52 images collected in four independent experiments. 28 of these images were collected at 30 min after mating, and all showed evidence of IC69 binding along the entire length of mutant axonemes. Therefore, the binding of IC69 to the axonemes during structural and functional rescue of outer dynein arms in *oda*2–wild-type dikaryons occurred along

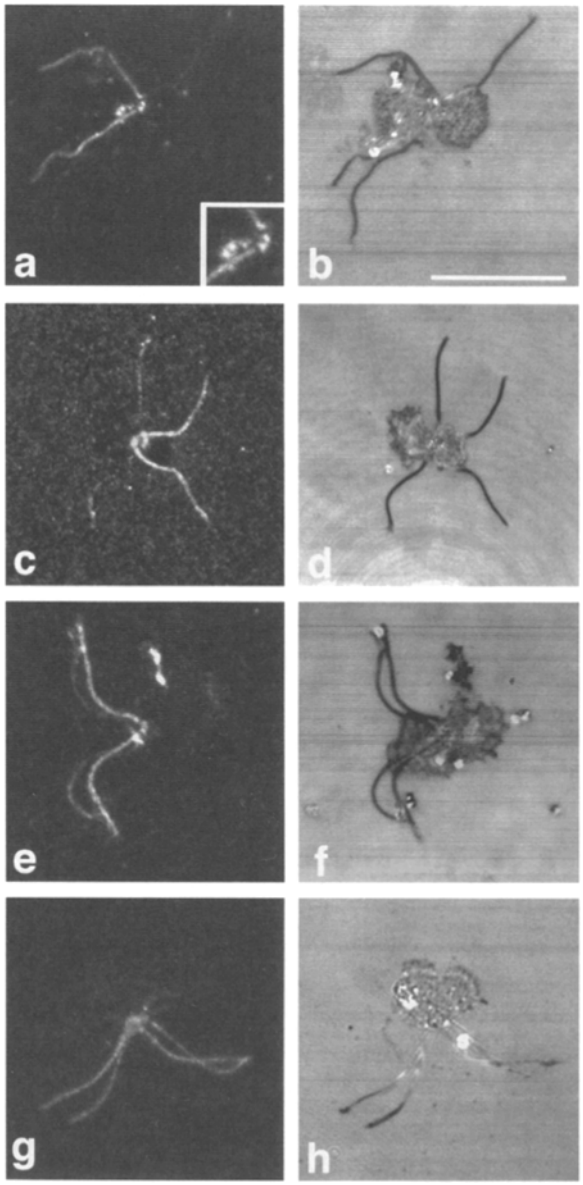

Figure 3. Immunofluorescence staining of *ida*4–wild-type dikaryons developing at 32°C by antibodies specific for p28. Dikaryons analyzed at 6 min (*a* and *b*), 20 min (*c* and *d*), 30 min (*e* and *f*), and 60 min after mating (*g* and *h*). Immunofluorescent images (*a*, *c*, *e*, and *g*) and corresponding reflectance images (*b*, *d*, *f*, and *h*). Inset in *a* shows the basal bodies at ~×2. Bar, 10 μm.

the entire length of axonemes without forming a concentration gradient at the distal part.

Results obtained with the analysis of *oda*6–wild-type dikaryons were similar to those of Fig. 4 (not shown). This was expected because structural rescue in both *oda*2–wild-type and *oda*6–wild-type dikaryons occurred by the assembly of whole outer dynein arms formed by wild-type proteins (20). Rescue of outer dynein arms in outer dynein mutants representing different loci is independent from the defective gene product (11).

Active Transport of p28 by KHP1

The dynein subunits p28 and IC69 could be transported to their binding site along the axoneme by passive diffusion

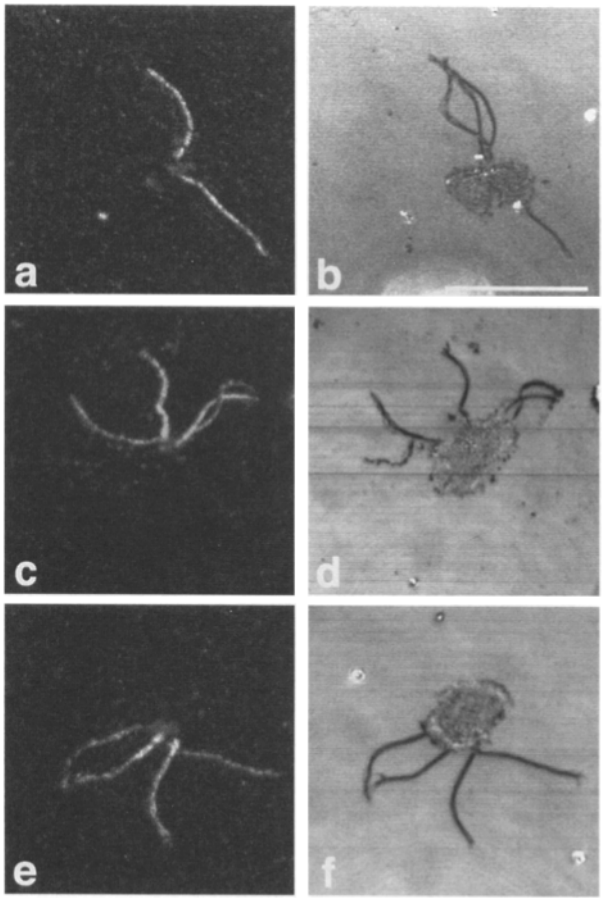

Figure 4. Immunofluorescence staining of *oda2*–wild-type dikaryons developing at 32°C by the antibodies specific for IC69. Dikaryons analyzed at 6 min (*a* and *b*), 30 min (*c* and *d*), and 60 min after mating (*e* and *f*). Immunofluorescent images (*a*, *c*, and *e*) and corresponding reflectance images (*b*, *d*, and *f*). Bar, 10 μm.

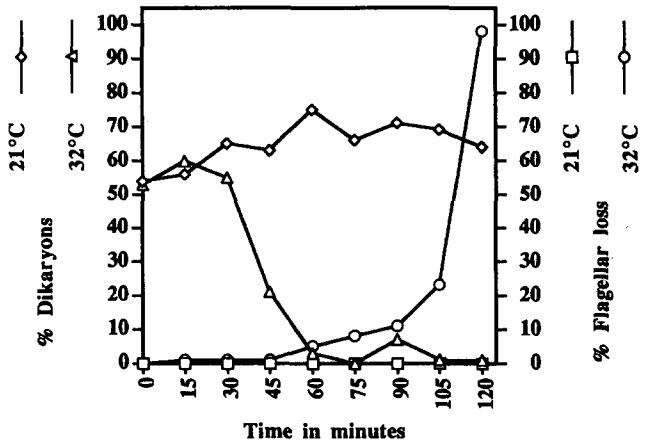

Figure 5. Diagram representing percentage of dikaryons that were formed (*left ordinate*) and percentage of cells losing their flagella (*right ordinate*) as a function of time. Dikaryons formed between *ida4fla10* and *fla10* gametes at 32°C (*triangles*) and 21°C (*diamonds*). Opposite mating types were mixed together at time 0. *ida4fla10* and *fla10* gametes and *ida4fla10-fla10* dikaryons losing their flagella at 32°C (*circles*) and 21°C (*squares*). Each point represents the average of three independent measurements.

or active transport. If they are actively transported, they could be carried by a molecular motor directed toward the plus end of microtubules, such as a kinesin-like protein.

To determine whether KHP1, the kinesin homologous protein associated with the *Chlamydomonas* outer doublet microtubules (33), is the molecular motor responsible for the active transport of p28 and IC69 in flagella, we created the recombinant strains *ida4fla10* and *oda2fla10* and analyzed the *ida4fla10-fla10* and *oda2fla10-fla10* dikaryons by specific antibodies and immunofluorescent microscopy.

The strain *fla10* is a temperature-sensitive mutant of KHP1. Therefore, at the permissive temperature of 21°C, the transport of dynein subunits to the distal end of the axonemes should occur in the *ida4fla10-fla10* and *oda2fla10-fla10* dikaryons, as observed in the *ida4*–wild-type and *oda2*–wild-type dikaryons (Figs. 3 and 4, respectively). In contrast, at the nonpermissive temperature of 32°C, the transport of dynein subunits should be inhibited, if it depends on the activity of KHP1.

The conditions adopted to perform the analysis of the dikaryons were chosen on the basis of the experiment shown in Fig. 5 and the following three criteria: first, the exposure of *ida4fla10*, *oda2fla10*, and *fla10* gametes at the nonpermissive temperature, 32°C, must precede the mating to inactivate the KPH1 protein. Second, the assembly of the dyneins along the full length of the axonemes requires ~1 h, as shown in Figs. 3 and 4. Third, the exposure at 32°C must be shorter than 2 h because after that time interval, the *fla10* mutation causes the loss of flagella.

Percentages of *ida4fla10-fla10* dikaryons and percentages of flagellar loss in *ida4fla10-fla10* dikaryons and *ida4fla10* and *fla10* gametes were measured as a function of time after exposure at 21° and 32°C (Fig. 5). At 32°C, the percentage of mating of *ida4fla10* gametes with *fla10* gametes remained constant for ~30 min and then dropped to close to zero within the following 30 min (Fig. 5, *triangles*), whereas at 21°C, the percentage of mating remained approximately constant for 2 h (Fig. 5, *diamonds*). Furthermore, at 32°C, *ida4fla10-fla10* dikaryons and *ida4fla10* and *fla10* gametes began to lose their flagella after 45 min of exposure, and all lost the flagella within 2 h (Fig. 5, *circles*), whereas at 21°C, they did not lose their flagella (Fig. 5, *squares*).

From the evidence shown in Fig. 5, we drew two conclusions. First, the mating of *ida4fla10* or *oda2fla10* gametes with *fla10* gametes should be performed between 30 and 60 min after the exposure at 32°C to detect an effect of the inactivation of the *fla10* gene product. Second, decrease of mating of *ida4fla10* gametes with *fla10* gametes at 32°C is independent from the loss of flagella because the curves representing mating and loss of flagella at 32°C intersect in their lowest parts. Therefore, KHP1 activity is also required for aspects of mating that do not involve flagella.

Before mating the *ida4fla10* gametes with *fla10* gametes, we first exposed them at 21° or 32°C for 45 min. We collected aliquots of cells at 6, 30, and 60 min after mating and performed immunofluorescence microscopy of dikaryons by labeling with antibodies specific for p28. The immunofluorescence of *ida4fla10-fla10* dikaryons from gametes exposed at 21°C (Fig. 6), was not significantly different from that observed for *ida4*–wild-type dikaryons (Fig. 3).

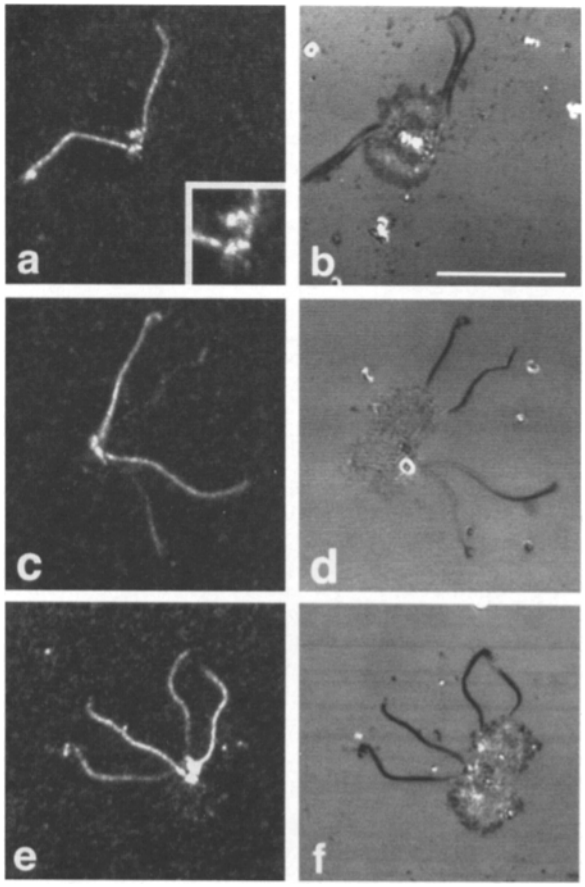

Figure 6. Immunofluorescence staining of *ida4fla10-fla10* dikaryons developing at 21°C by antibodies specific for p28. Dikaryons analyzed at 6 min (*a* and *b*), 30 min (*c* and *d*), and 60 min after mating (*e* and *f*). Immunofluorescent images (*a*, *c*, and *e*) and corresponding reflectance images (*b*, *d*, and *f*). Inset in *a* shows the staining of two couples of basal bodies at ~×2. Bar, 10 μm.

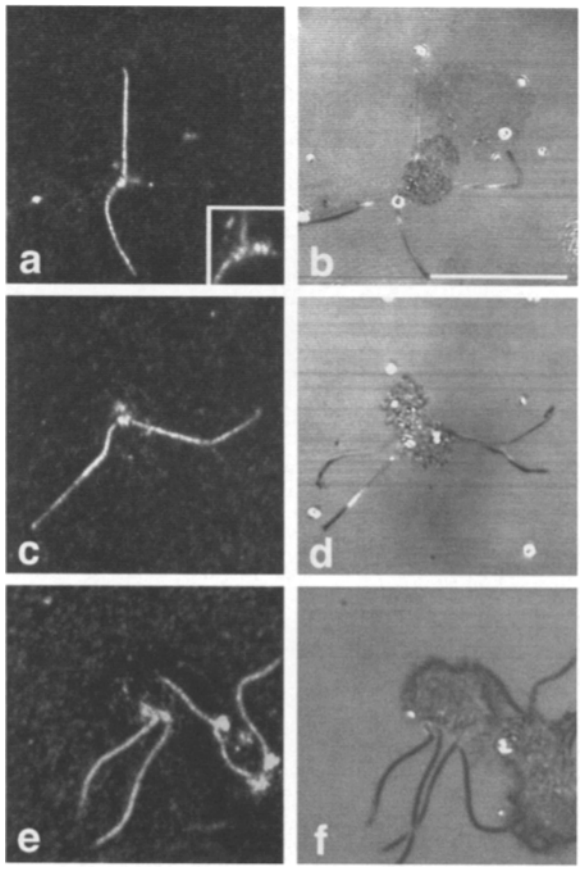

Figure 7. Immunofluorescence staining of *ida4fla10-fla10* dikaryons developing at 32°C by antibodies specific for p28. Dikaryons analyzed at 6 min (*a* and *b*), 30 min (*c* and *d*), and 60 min after mating (*e* and *f*). Immunofluorescent images (*a*, *c*, and *e*) and corresponding reflectance images (*b*, *d*, and *f*). Inset in *a* shows the basal bodies at ~×2. Bar, 10 μm.

At 6 min after mating, one pair of axonemes and two pairs of basal bodies were stained (Fig. 6 *a* and *inset*). At 30 min, the distal but not the proximal part of mutant axonemes was stained with decreasing intensity from distal to proximal parts (Fig. 6 *c*). Within 60 min, the structural rescue of mutant axonemes was nearly complete (Fig. 6 *e*), as assessed by labeling with the antibodies to p28 along the length of mutant axoneme.

The immunofluorescence of *ida4fla10-fla10* dikaryons from gametes exposed at 32°C showed that the binding of the antibodies occurred on only one pair of axonemes and two pairs of basal bodies at each time point (Fig. 7, *a*, *c*, and *e*). The binding of p28 along mutant axonemes did not occur after 30 min (Fig. 7 *c*), and it was reduced to a trace after 60 min (Fig. 7 *e*). The images shown in Figs. 6 and 7 were selected as typical examples of the 64 images collected in three independent experiments. 26 of these images were collected at 30 or 60 min after mating at 32°C. They all showed that the binding of p28 was not rescued in mutant axonemes.

These observations indicate that KHP1 is required for p28 transport to the distal part of axonemes but not for p28 transport to the basal bodies.

The 45-min time interval chosen for the exposure of *ida4-fla10* and *fla10* gametes before mating at the restrictive temperature is critical. Dikaryons obtained with *ida4fla10* and *fla10* gametes after 30 min exposure at 32°C (not shown) had p28 located at the distal part of the axoneme in lower amounts than those observed at 21°C (Fig. 6 *c*). Furthermore, *ida4fla10* and *fla10* gametes after 50 min of exposure at 32°C either did not generate dikaryons or generated dikaryons that subsequently lost their flagella (not shown).

Transport of IC69 Does Not Require the Activity of KHP1

Experiments performed by a procedure identical to that described above were developed for *oda2fla10* and *fla10* gametes and the antibodies specific for IC69, the outer dynein arm intermediate chain. Dikaryons were obtained by mating gametes exposed at 21° or 32°C for 45 min. The immunofluorescence of *oda2fla10-fla10* dikaryons obtained at 21°C (not shown) or 32°C (Fig. 8, *a*, *c*, and *e*) was similar to that observed for *oda2*–wild-type dikaryons (Fig. 4). The binding of IC69 to the pair of mutant axonemes was undetectable at 6 min after mating (Fig. 8 *a*), but it was evident at 30 min (Fig. 8, *c* and *e*). Both distal and proximal parts of the axonemes were stained with similar intensities (Fig. 8, *c* and *e*). The images shown in Fig. 8 were selected

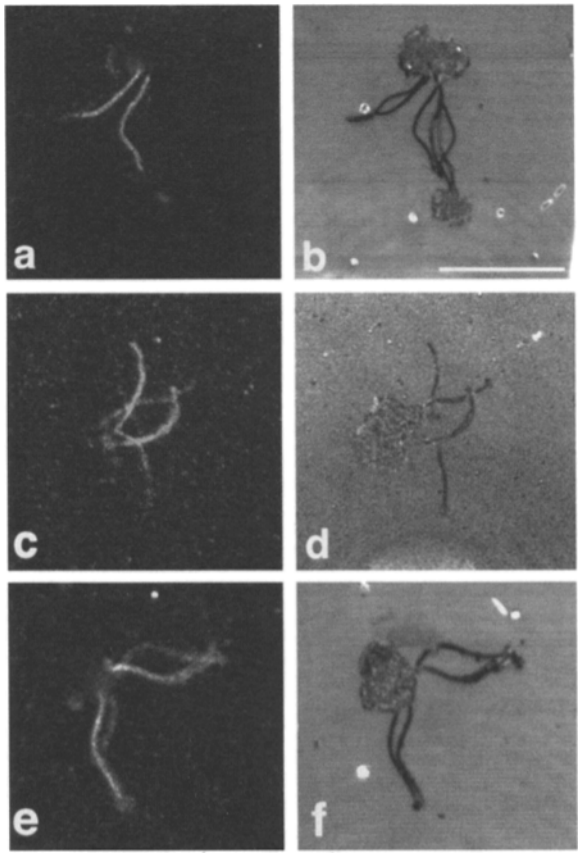

Figure 8. Immunofluorescence staining of *oda2fla10-fla10* dikaryons developing at 32°C by the antibodies specific for IC69. Dikaryons analyzed at 6 min (*a* and *b*) and 30 min after mating (*c–f*). Immunofluorescent images (*a*, *c*, and *e*) and corresponding reflectance images (*b*, *d*, and *f*). Bar, 10 μm.

as typical examples of the 44 images collected in four independent experiments. 28 of these images were collected at 30 min after mating at 32°C. They all showed evidence of IC69 binding along the entire length of mutant axonemes. Therefore, the assembly of IC69 along mutant axonemes does not require the activity of KHP1.

Discussion

We report here an analysis of the rescue of dynein arms in mutant axonemes, as it occurs in dikaryons that were formed by a wild-type strain and a dynein mutant. The same experimental approach was used before to identify the site of assembly of radial spoke structures to outer doublet microtubules (9). We also used dikaryons as an experimental system to identify mutant gene products within the axoneme (21). All these analyses benefited from the fact that the defects of mutant flagella can be rescued by a wild-type axonemal precursor after the formation of dikaryons (21).

Transport of inner and outer dynein precursors in mutant flagella of dikaryons occurred independently from flagellar growth and toward binding sites that remained available as a consequence of a mutation. In contrast, transport and binding of the majority of dynein arms in wild-type flagella occur simultaneously to flagellar growth. Nevertheless, transport mechanisms and binding of dyneins to outer doublet microtubules should be similar in both systems, mutant flagella of dikaryons and developing wild-type flagella.

We observed the rescue of p28, an inner dynein arm light chain, or the rescue of IC69, an outer dynein arm intermediate chain in *ida4*–wild-type or in *oda2*–wild-type dikaryons, respectively. Furthermore, we assumed that the whole dyneins containing these subunits were rescued. The rescue of outer dynein arms in flagella of four outer dynein arm mutants, including *oda2*, involved the complete set of outer dynein arm subunits from wild-type gametes (20). The rescue of inner dynein arms in *ida4* flagella required coassembly of inner dynein arm subunits from both wild-type and mutant gametes (17).

We solubilized the cell wall and extracted the resulting protoplasts by glycerol and a detergent before exposing them to the antibodies. Therefore, our microscopic analysis was limited to antigens bound to insoluble structures. The use of confocal microscopy provided us with the sensitivity and resolution needed to determine the relative position of inner or outer dynein arms in focal planes containing the whole axoneme. We were able to observe asymmetric or symmetric location of antigens along mutant axonemes of the dikaryons. These signals were generated by the assembly of dynein arms progressively from the distal part of the axoneme or homogeneously all along its entire length during the rescue.

Inner dynein arms containing p28 and outer dynein arms were transported and bound to mutant axonemes of dikaryons in different orders. The first bound from the distal part and were extended toward the proximal part of the axoneme forming a concentration gradient, whereas the second bound along the entire length of the axoneme with no initial preference for the distal part.

Structural rescue of inner dynein arms containing p28 in dikaryons required the completion of the following events: first, the transport of inner dynein arms to the distal end of the axoneme; second, the transport of the same arms to their specific sites inside the axonemal shaft; and finally, the binding of the arms to their sites.

We showed in the Results section that the transport of inner dynein arms containing p28 to the distal end of the axonemes requires the activity of KHP1, kinesin homologue protein (33). The existence of a transport to the distal part of the axoneme was postulated before, although neither an active transport nor a molecular motor was identified (10). Both transport of inner dynein arms to the distal part of the axoneme and bidirectional movement of granule-like particles beneath the flagellar membrane (14) require the activity of KHP1. However, a direct interaction of KHP1 with either p28 or the granule-like particles remains to be determined.

The transport of inner dynein arms to the distal part of the axonemes probably occurs between the outer doublet microtubules and the flagellar membrane where inner dynein arm binding sites are not available (29). Simultaneous presence of inner dynein arms and inner dynein arm binding sites within the axonemal shaft would have favored an assembly from the proximal and toward the distal part, if the inner dynein arms from the cell body are directly

transported inside the axoneme. This interpretation also is in agreement with the evidence that the KHP1 protein is located in the region between the outer doublet microtubules and the flagellar membrane (15).

Our previous observations of the binding of inner dynein arms during flagellar regeneration revealed that two inner dynein arm heavy chains, including one that binds p28, are assembled at the end of flagellar development and are located at the proximal part of the axoneme (26). Therefore, these precursors after being transported to the distal part of the axoneme reach their final binding site inside the axonemal shaft by a second mechanism involving regulation in time and space. This mechanism may also require active transport involving a molecular motor directed to the minus end of microtubules, like the dyneins. Ultimately, these proximal and late-assembled inner dynein arms may transport themselves to their final destination.

Observations obtained by Johnson and Rosenbaum (9) revealed that tubulin and radial spoke subunits are assembled at the distal part of the axoneme like the inner dynein arms containing p28. Nevertheless, the necessity of distal assembly for tubulin or radial spoke or inner dynein arm subunits may have different reasons. The microtubules are asymmetric structures and preferentially grow at their plus end located at the distal part of the axoneme. In contrast, radial spokes and inner dynein arms are appendages to the microtubules and must penetrate the internal part of the axonemal shaft to bind to the outer doublet microtubules.

We can make a distinction between axonemal precursors that are transported by the kinesin homologous protein, KHP1, as the inner dynein arm containing p28, and axonemal precursors that are not, as the outer dynein arms. The difference may be a consequence of the final destination of the precursors in the axonemal shaft. Those like the inner dynein arms that are located at the interior of the axonemal shaft may require active transport by KHP1. Other precursors, like the outer dynein arms, which are at the exterior part of the axoneme, or tubulin, which forms the axonemal shaft, may diffuse to their binding site or be transported by molecular motors other than KHP1. Some of these hypotheses can be tested. For instance, transport of central complex and radial spoke precursors to the distal part of the axoneme may require the activity of KHP1.

Our observations do not exclude a binding of outer dynein arms at the distal end of developing wild-type flagella, like the binding of the majority of axonemal proteins (35). Staining of the entire length of mutant axonemes and absence of a concentration gradient of outer dynein arms either at the distal or proximal parts of axonemes during the rescue in dikaryons suggests that the mechanism of binding of outer dynein arms to the outer doublet microtubules is much slower than the mechanism of transport. This delay may be a consequence of the existence of a complex mechanism of binding. An HSP70 chaperone was identified at the distal part of *Chlamydomonas* axoneme and could participate in the binding of different substructures to the outer doublet microtubules (3).

The activity of KHP1 is not required for the assembly of the p28-like protein to the basal bodies. Therefore, axonemal precursors are distinguished from basal body precursors and are transported to their specific binding sites. This sorting mechanism may exist for a variety of axonemal precursors. Other molecules, like actin (25), caltractin/centrin (8), and calmodulin (32), are located in the axoneme as well as in other cytoskeletal frameworks.

The KHP1 proteins themselves may be sorted and transported to different cellular compartments. Genetic evidence suggested that KHP1 interacts with multiple components of the flagellar apparatus and is involved in the cell cycle (22). Furthermore, our own observations suggested that molecular events occurring in cellular compartments other than flagella involve KHP1 in the mating process. Differentiation of the plasma membrane and cell fusion of gametes of opposite mating types precede the formation of quadriflagellate dikaryons and may require the activity of KHP1.

The presence of a p28-like protein in the basal bodies is surprising because basal bodies do not contain inner dynein arms. On the other hand, other inner dynein arm light chains, caltractin/centrin and actin, have different locations and functions in *Chlamydomonas* cells. Caltractin/centrin is present in the transition zone between axonemes and basal bodies and is involved in the calcium-dependent excision of the flagellar shaft from the basal bodies (30). Actin forms filaments in the fertilization tubule of gametes before cell fusion (5). Therefore, dynein light chains and homologous basal body components may have different functions.

Our observation that a mutation in the *IDA4* locus affects the binding of p28 to both axonemes and basal bodies suggests that the basal bodies could be a site of processing for axonemal precursors that are actively transported by KHP1 toward the axoneme. Observations supporting this hypothesis could be easily obtained: KHP1 and radial spoke subunits could be components of the basal bodies, as observed for p28. Interestingly, in the article published by Johnson and Rosenbaum (9) about the assembly of radial spokes within the axoneme, several images obtained by antibodies specific for two radial spoke subunits show immunofluorescent staining of the basal body region of the cell.

The observation that only a subset of axonemal substructures depends on the same mechanism of transport stimulates a variety of questions concerning targeting of the axonemal molecules, association with and dissociation from molecular motors, transport of molecules from a distal to a proximal position, and, finally, binding to sites located in asymmetric positions along and around the axoneme. Many of these questions can be answered by experimental approaches similar to those described here. Furthermore, the analysis of temperature-dependent assembly mutants other than *fla*10 (1, 7) may reveal additional features of flagellar assembly.

We are grateful to Michel LeDizet (University of California, San Francisco) for a critical reading of this manuscript.

This work was supported by a grant from the National Institutes of Health (GM-44467).

Received for publication 19 December 1995 and in revised form 31 January 1996.

References

1. Adams, G.M.W., B. Huang, and D.J.L. Luck. 1982. Temperature-sensitive

assembly-defective flagella mutants of *Chlamydomonas reinhardtii*. *Genetics*. 100:579–586.
2. Amos, L.A., and W.B. Amos. 1991. The bending of sliding microtubules imaged by confocal light microscopy and negative stain electron microscopy. *J. Cell Sci. Suppl.* 14:95–101.
3. Bloch, M.A., and K.A. Johnson. 1995. Identification of a molecular chaperone in the eukaryotic flagellum and its localization to the site of microtubule assembly. *J. Cell Sci.* 108:3541–3545.
4. Brokaw, C.J., and R. Kamiya. 1987. Bending patterns of *Chlamydomonas* flagella: IV. Mutants with defects in inner and outer dynein arms indicate differences in dynein arm function. *Cell Motil. Cytoskeleton.* 8:68–75.
5. Detmers, P.A., U.W. Goodenough, and J. Condeelis. 1983. Elongation of the fertilization tubule in *Chlamydomonas*: new observations on the core microfilaments and the effect of transient intracellular signals on their structural integrity. *J. Cell Biol.* 97:522–532.
6. Harris, E.H. 1989. The *Chlamydomonas* Sourcebook. Academic Press, New York. 780 pp.
7. Huang, B., M.R. Rifkin, and D.J. Luck. 1977. Temperature-sensitive mutations affecting flagellar assembly and function in *Chlamydomonas reinhardtii*. *J. Cell Biol.* 72:67–85.
8. Huang, B., A. Mengersen, and V.D. Lee. 1988. Molecular cloning of cDNA for caltractin, a basal body-associated Ca^{2+}-binding protein: homology in its protein sequence with calmodulin and the yeast *CDC31* gene product. *J. Cell Biol.* 107:133–140.
9. Johnson, K.A., and J.L. Rosenbaum. 1992. Polarity of flagellar assembly in *Chlamydomonas*. *J. Cell Biol.* 119:1605–1611.
10. Johnson, K.A., and J.L. Rosenbaum. 1993. Flagellar regeneration in *Chlamydomonas*: a model system for studying organelle assembly. *Trends Cell Biol.* 3:156–161.
11. Kamiya, R. 1988. Mutations at twelve independent loci result in absence of outer dynein arms in *Chlamydomonas reinhardtii*. *J. Cell Biol.* 107:2253–2258.
12. King, S.J., W.B. Inwood, E.T. O'Toole, J. Power, and S.K. Dutcher. 1994. The *bop2-1* mutation reveals radial asymmetry in the inner dynein arm region of *Chlamydomonas reinhardtii*. *J. Cell Biol.* 126:1255–1266.
13. King, S.M., T. Otter, and G.B. Witman. 1985. Characterization of monoclonal antibodies against *Chlamydomonas* flagellar dynein. *Proc. Natl. Acad. Sci. USA*. 82:4717–4721.
14. Kozminski, K.G., K.A. Johnson, P. Forscher, and J.L. Rosenbaum. 1993. A motility in the eukaryotic flagellum unrelated to flagellar beating. *Proc. Natl. Acad. Sci. USA*. 90:5519–5523.
15. Kozminski, K.G., P.L. Beech, and J.L. Rosenbaum. 1995. The *Chlamydomonas* kinesin-like protein *FLA*10 is involved in motility associated with the flagellar membrane. *J. Cell Biol.* 131:1517–1527.
16. LeDizet, M., and G. Piperno. 1986. Cytoplasmic microtubules containing acetylated α-tubulin in *Chlamydomonas reinhardtii*: spatial arrangement and properties. *J. Cell Biol.* 103:13–22.
17. LeDizet, M., and G. Piperno. 1995. *ida4*-1, *ida4*-2 and *ida4*-3 are intron splicing mutations affecting the locus encoding p28, a light chain of *Chlamydomonas* axonemal inner dynein arms. *Mol. Biol. Cell.* 6:713–723.
18. LeDizet, M., and G. Piperno. 1995. The light chain p28 associates with a subset of inner dynein arm heavy chains in *Chlamydomonas* axonemes. *Mol. Biol. Cell.* 6:697–711.
19. Luck, D.J.L. 1984. Genetic and biochemical dissection of the eucaryotic flagellum. *J. Cell Biol.* 98:789–794.
20. Luck, D.J.L., and G. Piperno. 1989. Dynein arm mutants of *Chlamydomonas*. *In* Cell Movement. Vol. 1. F.D. Warner, P. Satir, and I.R. Gibbons, editors. Alan R. Liss, New York. 49–60.
21. Luck, D., G. Piperno, Z. Ramanis, and B. Huang. 1977. Flagellar mutants of *Chlamydomonas*: studies of radial spoke-defective strains by dikaryon and revertant analysis. *Proc. Natl. Acad. Sci. USA*. 74:3456–3460.
22. Lux, F.G., and S.K. Dutcher. 1991. Genetic interactions at the *FLA*10 locus: suppressors and synthetic phenotypes that affect the cell cycle and flagellar function in *Chlamydomonas reinhardtii*. *Genetics*. 128:549–561.
23. Mitchell, D.R., and Y. Kang. 1991. Identification of *oda6* as a *Chlamydomonas* dynein mutant by rescue with the wild-type gene. *J. Cell Biol.* 113:835–842.
24. Pawley, J.B. 1990. Handbook of Biological Confocal Microscopy. Plenum Press, New York. 232 pp.
25. Piperno, G., and D.J. Luck. 1979. An actin-like protein is a component of axonemes from *Chlamydomonas* flagella. *J. Biol. Chem.* 254:2187–2190.
26. Piperno, G., and Z. Ramanis. 1991. The proximal portion of *Chlamydomonas* flagella contains a distinct set of inner dynein arms. *J. Cell Biol.* 112: 701–709.
27. Piperno, G., Z. Ramanis, E.F. Smith, and W.S. Sale. 1990. Three distinct inner dynein arms in *Chlamydomonas* flagella: molecular composition and location in the axoneme. *J. Cell Biol.* 110:379–389.
28. Piperno, G., K. Mead, and W. Shestak. 1992. The inner dynein arms I2 interact with a "dynein regulatory complex" in *Chlamydomonas* flagella. *J. Cell Biol.* 118:1455–1463.
29. Piperno, G., K. Mead, M. LeDizet, and A. Moscatelli. 1994. Mutations in the "dynein regulatory complex" alter the ATP-insensitive binding sites for inner arm dyneins in *Chlamydomonas* axonemes. *J. Cell Biol.* 125: 1109–1117.
30. Sanders, M.A., and J.L. Salisbury. 1989. Centrin-mediated microtubule severing during flagellar excision in *Chlamydomonas reinhardtii*. *J. Cell Biol.* 108:1751–1760.
31. Snell, W.J., W.L. Dentler, L.T. Haimo, L.I. Binder, and J.L. Rosenbaum. 1974. Assembly of chick brain tubulin onto isolated basal bodies of *Chlamydomonas reinhardtii*. *Science (Wash. DC)*. 185:357–360.
32. Van Eldik, L.J., G. Piperno, and D.M. Watterson. 1980. Similarities and dissimilarities between calmodulin and a *Chlamydomonas* flagellar protein. *Proc. Natl. Acad. Sci. USA*. 77:4779–4783.
33. Walther, Z., M. Vashishtha, and J.L. Hall. 1994. The *Chlamydomonas* *FLA10* gene encodes a novel kinesin-homologous protein. *J. Cell Biol.* 126:175–188.
34. Wilkerson, C.G., S.M. King, and G.B. Witman. 1994. Molecular analysis of the γ heavy chain of *Chlamydomonas* flagellar outer-arm dynein. *J. Cell Sci.* 107:497–506.
35. Witman, G.B. 1975. The site of in vivo assembly of flagellar microtubules. *Ann. NY Acad. Sci.* 253:178–191.